Supporting Information

Twist and return – induced ring strain triggers quick relaxation of a (*Z*)-stabilized cyclobisazobenzene

Chavdar Slavov,[#,1] Chong Yang,[#,2], Andreas H. Heindl,[3] Tim Stauch[2,‡], Hermann A. Wegner,[3] Andreas Dreuw,[,2] and Josef Wachtveitl[*,1].*

[1]Institute of Physical and Theoretical Chemistry, Goethe University, Frankfurt, Germany

[2]Interdisciplinary Center for Scientific Computing (IWR), University of Heidelberg, Heidelberg, Germany

[3]Institute of Organic Chemistry, Justus Liebig University, Giessen, Germany

AUTHOR INFORMATION

Corresponding Author

* e-mail: wveitl@theochem.uni-frankfurt.de

* e-mail: dreuw@uni-heidelberg.de

[#]These authors contributed equally to this work.

[‡]Present address: Department of Chemistry, University of California, Berkeley, USA

Experimental methods

Femtosecond transient absorption

The cyclobisazobenzene, *(Z,Z)*-CBA, was prepared as previously described[1] and dissolved in ethanol for the spectroscopic experiments. The stationary absorption spectra were recorded on a Specord S600, Analytik Jena spectrophotometer. The fs transient absorption set-up used for the time-resolved experiments was described previously.[2] In short, it consists of an oscillator/amplifier system (Clark, MXR-CPA-iSeries, 775 nm, 150 fs, 1 kHz). The pump pulses at 304 nm and 437 nm were generated via sum frequency mixing of the pulses from a home-built two stage NOPA (noncollinear optical parametric amplifier)[3-4] and the laser fundamental. The probe pulses (single filament white light, 300-700 nm) were generated by focusing the laser fundamental in a CaF_2 crystal (5 mm). The signal detection was done in reference mode by two spectrometers (600 lines/mm gratings, blazed at 300 nm, and a 64-channel photodiode array). The experiments were performed under magic angle conditions (54.7° pump-probe polarization angle difference) to eliminate anisotropic contributions. A prism compressor placed between the two NOPA stages was used to compress the NOPA pulses. The final pump-probe cross-correlation was ~100-120 fs. A fused silica cuvette with 1 mm optical path length was used for the experiments.

Flash photolysis experiments

Flash photolysis measurements were performed to determine the thermal $E \rightarrow Z$ back isomerization rate of CBA. The home-built flash photolysis set-up is based on a nanosecond Nd:YAG laser (1064 nm, Spitlight 600, Innolas Laser GmbH), which pumps an optical parametric oscillator (preciScan; GWU-Lasertechnik, Erftstadt, Germany) to generate nanosecond excitation pulses of 430 nm.[5] The probe pulses are provided by a spectrally broad xenon flash lamp (2.9 μs pulses, L7685, Hamamatsu). The detection system (~0.5 nm spectral resolution) is composed of a spectrograph (Acton SP2150, Princeton Instruments) and an ICCD camera (PIMAX 3, Princeton Instruments). The experimental datasets were binned to a final wavelength resolution of ~2 nm.

Data analysis

The time-resolved data were analyzed by lifetime distribution analysis (LDA) using OPTIMUS (www.optimusfit.org) as detailed in [6]. LDA is a model independent type of data analysis that naturally deals with non-exponential or stretched exponential kinetics. In this analysis the pre-exponential amplitudes in a sum of a large number (100) of exponential functions with fixed, equally spaced (on a decimal logarithm scale) lifetimes are determined. The obtained pre-exponential amplitudes at each detection wavelength can be presented in the form of a contour lifetime density map (LDM).

The coherent artifact contribution at time zero position in the ultrafast transient absorption experiments was approximated with a function composed of a Gaussian and/or its first and second derivative[7] and fitted within the same routine as the LDA.

Theoretical methods

Time-dependent density functional calculations

The quantum chemical calculations were performed using time-dependent density functional theory (TD-DFT)[8-10] with the BHLYP functional[11], 6-31G* basis set[12], and a conductor-like polarizable continuum model (C-PCM)[13-15] for ethanol solvation (dielectric constant of $\varepsilon = 24.5$). Note that a ~35 nm shift exists between the calculated bright vertical excited state of *(Z,Z)*-CBA and its experimental absorption peak. The BHLYP functional was chosen, since it exhibits a reasonable agreement with the experimental data, and in addition has a substantial amount of non-local orbital exchange, which is required in such multichromophoric systems to alleviate the known charge-transfer problem of TDDFT[10]. In particular, since excited-state geometry optimizations are to be performed, xc-functionals with low amounts of non-local exchange lead to artificial CT minima on the potential energy surfaces (PES).[16]

The absorption spectra of CBA in (*Z,Z*)-, (*Z,E*)-, (*E,E*)-CBA (Fig. S2) were calculated for two possible ground state geometries (CBA-1 and CBA-2) in each isomerization state (Fig. S1). In case of (*E,E*)-CBA, the two structures correspond to enantiomers with identical physical and optical properties, while in (*Z,E*)- and (*Z,Z*)-CBA they are truly different. The vertical excitation energies and the potential energy curves were calculated by TDDFT at the same level of theory to explore the isomerization mechanism of CBA. The relaxed S_1, S_2, S_3 PES were calculated by scanning the PESs along the torsional coordinate based on optimized geometries of the S_1, S_2, S_3 states, respectively. The Tamm-Dancoff approximation (TDA) was used in the TD-DFT calculations of relaxed PESs. All quantum chemical calculations for the CBA were carried out using the Q-Chem 4.4[17] and Orca 3.0[18] program packages.

Molecular strain analysis

The isodesmic reaction shown in Fig. S6 was used to quantify the strain in CBA. Isodesmic reactions are fictitious reaction schemes in which the number of each type of bond on each side of the equation is the same. The calculation of reaction Gibbs energy, ΔG, in such reactions allows the quantification of the strain in the functional groups and the entire molecule.[19-21] Each reactant and product in the isodesmic reaction contributes a term ΔG_i to the total Gibbs energy:

$$\Delta G_i = \Delta E_{DFT,i} + \Delta E_{ZPV,i} + \Delta H_i + T\Delta S_i$$

Here, $\Delta E_{DFT,i}$ is the total energy of the optimized molecule i at the BHLYP/6-31G* level of theory, $\Delta E_{ZPV,i}$ is its zero point vibrational energy, ΔH_i is its enthalpy, ΔS_i is its entropy and T is the temperature (298.15 K). All calculations reported here were

performed as described above. To calculate the total value of ΔG, the corresponding values of the reactants were subtracted from the values of the products. This procedure allows a comparison of the molecular strain in the different CBA isomers. Negative values of ΔG indicate strain in the reactants, while positive values indicate that the reactants are stabilized with respect to the products. The JEDI (Judgement of Energy DIstribution) analysis was used to gain further insights into the distribution of the strain energy in CBA.[22-23] JEDI is a quantum chemical tool that quantifies the strain energy in each internal coordinate of the molecule, *i.e.* each bond, bending and torsion. Based on the harmonic approximation, the energy contribution ΔE_i of each of the M internal coordinates of the molecule can be calculated via:

$$\Delta E_i = \frac{1}{2}\sum_{j}^{M} \left.\frac{\partial^2 V(\vec{q})}{\partial q_i \partial q_j}\right|_{\vec{q}=\overrightarrow{q_0}} \Delta q_i \Delta q_j$$

Where $\left.\frac{\partial^2 V(\vec{q})}{\partial q_i \partial q_j}\right|_{\vec{q}=\overrightarrow{q_0}}$ is the Hessian matrix in redundant internal coordinates and Δq_i is the change in internal coordinate *i* upon mechanical deformation. The total harmonic strain energy, ΔE_{harm}, in the molecule can be calculated by summing up all individual contributions ΔE_i. It is useful to compare ΔE_{harm} to the ΔG values from the isodesmic reactions as a check for consistency (see Table S2), since both quantities provide estimates for molecular strain.

To analyze the distribution of strain energy within the different isomers of CBA via the JEDI analysis, the molecules were split into two parts, each of which consists of the azobenzene moiety and a methyl group, thus representing one half of the total system. The reason for this approach is the requirement of the JEDI analysis to calculate the change in internal coordinates Δq between a relaxed and a mechanically strained geometry (see equation above). Splitting CBA in this manner allows to subsequently conduct an ordinary geometry optimization, thus generating the relaxed geometry, and to calculate Δq with respect to the geometry of the structure cut out of the entire system. The total strain energy can then be calculated by adding up the strain energy contributions from both parts of the molecule. This approach can be theoretically justified by arguing that each azobenzene moiety in CBA acts as a "tweezer", which mechanically compresses its counterpart.

The ΔG values, calculated via the isodesmic reactions, are strongly negative in all cases considered here (Table S2). The reason is that the *Z*-moieties of the different isomers of CBA are compared to unstrained *E*-isomers of derivatives of azobenzene (*cf.* Fig. S6), which of course leads to pronounced strain in the educts of the isodesmic reaction. The JEDI analysis, by contrast, considers only the additional strain due to the embedding of the azobenzene moiety in the CBA macrocycle, and hence demonstrates that strain in all (*Z*)-AB moieties in the various CBA isomers differ only insignificantly from the values in

monomeric (*Z*)-AB. Hence, isodesmic reactions and the JEDI analysis provide different points of view on the molecular strain in CBA.

(1) Heindl, A. H.; Schweighauser, L.; Logemann, C.; Wegner, H. A. Azobenzene Macrocycles: Synthesis of a Z-Stable Azobenzenophane. *Synthesis* **2017,** *49* (12), 2632.
(2) Slavov, C.*, et al.* Ultrafast coherent oscillations reveal a reactive mode in the ring-opening reaction of fulgides. *Phys. Chem. Chem. Phys.* **2015,** *17*, 14045.
(3) Wilhelm, T.; Piel, J.; Riedle, E. Sub-20-fs pulses tunable across the visible from a blue-pumped single-pass noncollinear parametric converter. *Opt. Lett.* **1997,** *22* (19), 1494.
(4) Riedle, E.*, et al.* Generation of 10 to 50 fs pulses tunable through all of the visible and the NIR. *Appl. Phys. B* **2000,** *71* (3), 457.
(5) Chatterjee, D.*, et al.* Influence of arrestin on the photodecay of bovine rhodopsin. *Angew. Chem. Int. Ed.* **2015,** *54*, 13555.
(6) Slavov, C.; Hartmann, H.; Wachtveitl, J. Implementation and evaluation of data analysis strategies for time-resolved optical spectroscopy. *Anal. Chem.* **2015,** *87* (4), 2328.
(7) Kovalenko, S. A.; Dobryakov, A. L.; Ruthmann, J.; Ernsting, N. P. Femtosecond spectroscopy of condensed phases with chirped supercontinuum probing. *Phys. Rev. A* **1999,** *59* (3), 2369.
(8) Runge, E.; Gross, E. K. U. Density-Functional Theory for Time-Dependent Systems. *Phys. Rev. Lett.* **1984,** *52* (12), 997.
(9) Casida, M. E. *Recent Advances in Density Functional Methods*. World Scientific: 1995; Vol. Part I.
(10) Dreuw, A.; Head-Gordon, M. Single-Reference ab Initio Methods for the Calculation of Excited States of Large Molecules. *Chem. Rev.* **2005,** *105* (11), 4009.
(11) Becke, A. D. A new mixing of Hartree–Fock and local density□functional theories. *J. Chem. Phys.* **1993,** *98* (2), 1372.
(12) Hehre, W. J.; Ditchfield, R.; Pople, J. A. Self—Consistent Molecular Orbital Methods. XII. Further Extensions of Gaussian—Type Basis Sets for Use in Molecular Orbital Studies of Organic Molecules. *J. Chem. Phys.* **1972,** *56* (5), 2257.
(13) Liu, J.; Liang, W. Analytical second derivatives of excited-state energy within the time-dependent density functional theory coupled with a conductor-like polarizable continuum model. *J. Chem. Phys.* **2013,** *138* (2), 024101.
(14) Liu, J.; Liang, W. Analytical approach for the excited-state Hessian in time-dependent density functional theory: Formalism, implementation, and performance. *J. Chem. Phys.* **2011,** *135* (18), 184111.
(15) Liu, J.; Liang, W. Analytical Hessian of electronic excited states in time-dependent density functional theory with Tamm-Dancoff approximation. *J. Chem. Phys.* **2011,** *135* (1), 014113.
(16) Plötner, J.; Dreuw, A. Pigment Yellow 101: A showcase for photo-initiated processes in medium-sized molecules. *Chem. Phys.* **2008,** *347* (1–3), 472.
(17) Shao, Y.*, et al.* Advances in molecular quantum chemistry contained in the Q-Chem 4 program package. *Mol. Phys.* **2015,** *113* (2), 184.
(18) Neese, F. The ORCA program system. *Comput. Molec. Sci.* **2012,** *2* (1), 73.
(19) Daoust, K. J.; Hernandez, S. M.; Konrad, K. M.; Mackie, I. D.; Winstanley, J.; Johnson, R. P. Strain Estimates for Small-Ring Cyclic Allenes and Butatrienes. *The Journal of Organic Chemistry* **2006,** *71* (15), 5708.

(20) Wheeler, S. E.; Houk, K. N.; Schleyer, P. v. R.; Allen, W. D. A Hierarchy of Homodesmotic Reactions for Thermochemistry. *J. Am. Chem. Soc.* **2009,** *131* (7), 2547.
(21) Stauch, T.; Günther, B.; Dreuw, A. Can Strained Hydrocarbons Be "Forced" To Be Stable? *J. Phys. Chem. A* **2016,** *120* (36), 7198.
(22) Stauch, T.; Dreuw, A. A quantitative quantum-chemical analysis tool for the distribution of mechanical force in molecules. *J. Chem. Phys.* **2014,** *140* (13), 134107.
(23) Stauch, T.; Dreuw, A. Quantum Chemical Strain Analysis For Mechanochemical Processes. *Acc. Chem. Res.* **2017,** *50* (4), 1041.

Table S1. Bond distances (Å), Bond angles (degrees) and Dihedral angles (degrees) of the optimized geometries of *(E)*- and *(Z)*-AB, *(Z,Z)*-, *(Z,E)* and *(E,E)*-CBA. The total energies (TE) are summarized in the table as well.

Structure	**∢CNNC [deg]**	**∢NNCC [deg]**	**∢CNN [deg]**	**R_{NN}**	**R_{NC}**	**TE (a.u.)**
***(E)*-AB**	179.9	0	115.5	1.23	1.41	
***(E)*-AB Expt. (X-ray)**	180	0	114.1	1.25	1.43	
***(Z)*-AB**	-7.9	-54.6	123.5	1.23	1.43	
***(Z)*-AB Expt. (X-ray)**	0	53.3	121.9	1.25	1.45	
***(Z,Z)*-CBA-1**	7.5/7.6	56.4/57.3	122.6/122.6	1.23/1.23	1.43/1.43	-1220.9854417165
***(Z,E)*-CBA-1**	11.5/146.6	53.5/-5.2	125.6/114.9	1.23/1.24	1.43/1.41	-1220.9579061554
***(E,E)*-CBA-1**	157.4/157.4	1.6/0.4	115.2/115.2	1.24/1.24	1.41/1.41	-1220.9634489785
***(Z,Z)*-CBA-2**	-7.5/-7.6	-56.5/-57.1	122.6/122.6	1.23/1.23	1.43/1.43	-1220.9854427800
***(Z,E)*-CBA-2**	-11.2/148.9	-52.8/6.5	114.2/125.7	1.23/1.24	1.43/1.41	-1220.9588884814
***(E,E)*-CBA-2**	-157.0/157.0	-2.1/1.7	115.4/115.3	1.24/1.24	1.41/1.41	-1220.9625889751

Table S2. CNNC dihedral angle, ΔG value of the isodesmic reaction, total strain energy ΔE_{harm} and strain energy in the dihedral angle ΔE_{CNNC} (kcal/mol and %) for the different investigated isomers of CBA. The quantities ΔE_{harm} and ΔE_{CNNC} were calculated with the JEDI analysis. The values for the *(Z,Z)*- and *(E,E)*-isomers are the sums of the individual contributions of each of the subunits, whereas the results for *(Z,E)*-CBA are split into contributions from the *(Z)*- and the *(E)*-isomers. Splitting the ΔG values, however, is not possible. The percentage of strain energy stored in the dihedral angle refers to the moiety under consideration (*i.e. (Z)* or *(E)*, respectively), not to the entire molecule.

Structure	**∢CNNC Z/E [deg]**	**ΔG [kcal/mol]**	**ΔE_{harm} Z/E [kcal/mol]**	**ΔE_{CNNC} Z/E [kcal/mol]**	**ΔE_{CNNC} Z/E [%]**
***(Z,Z)*-CBA-1**	7.6/-	-23.1	2.9/-	0/-	0/-
***(Z,E)*-CBA-1**	11.5/146.6	-40.1	2.4/28.0	0.2/8.4	8.8/30.1
***(E,E)*-CBA-1**	157.4/157.4	-36.8	-/35.2	-/7.4	-/21.0
***(Z,Z)*-CBA-2**	-7.5/	-23.1	3.3/-	0/-	0/-
***(Z,E)*-CBA-2**	-11.2/148.9	-39.5	2.7/25.7	0.2/6.7	6.7/26.2
***(E,E)*-CBA-2**	-157.0/157.0	-36.9	-/35.6	-/7.5	-/21.2

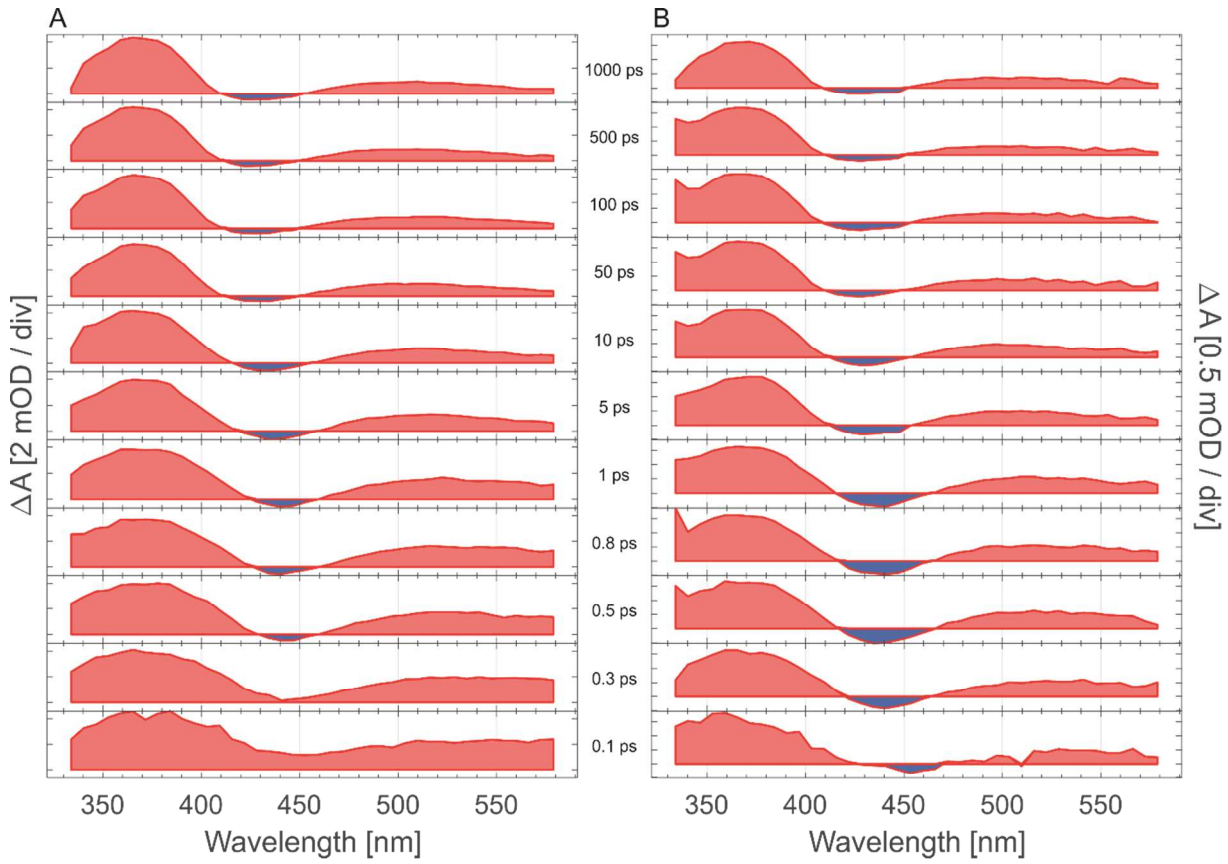

Figure S1. Transient spectra at selected points in time representing the spectral evolution of (Z,Z)-CBA in ethanol after 304 nm (A) and 437 nm (B) excitation.

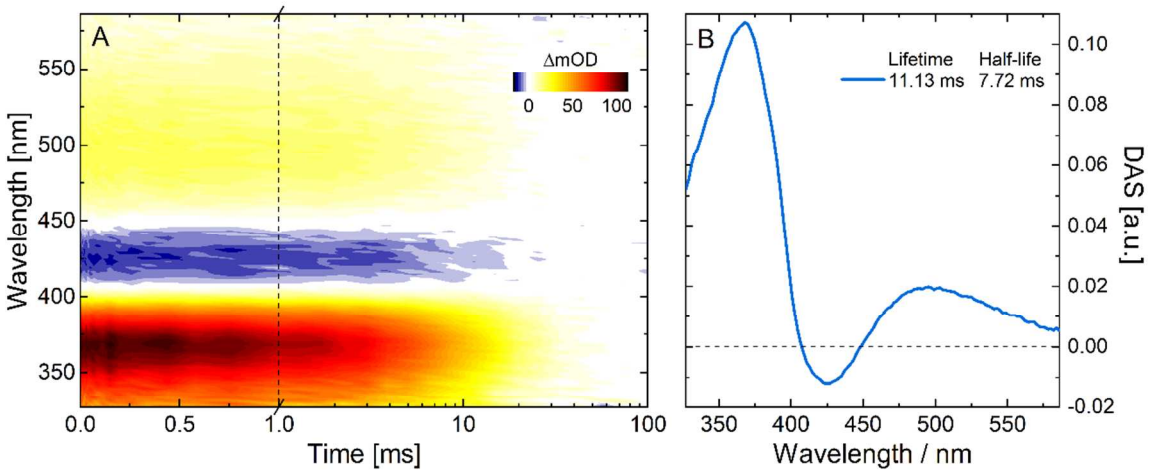

Figure S2. A) Transient absorption data recorded after 430 nm excitation of the *(Z,Z)*-CBA using nanosecond flash photolysis. B) Global analysis of the transient absorption data in A).

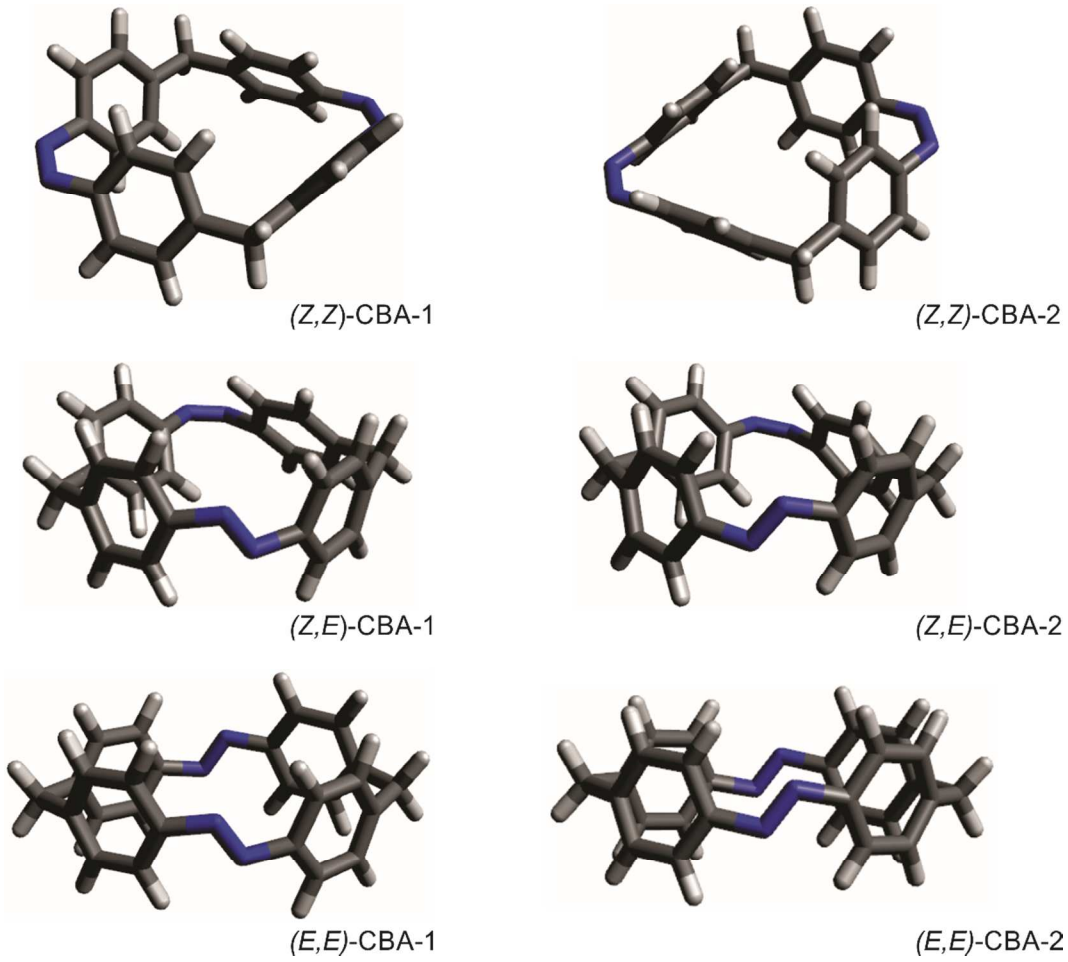

Figure S3. Geometry optimized structure of CBA. For each isomerization state, there are two different stable ground state geometries – CBA-1 and CBA-2 (see Table S1 for differences in the dihedral angles).

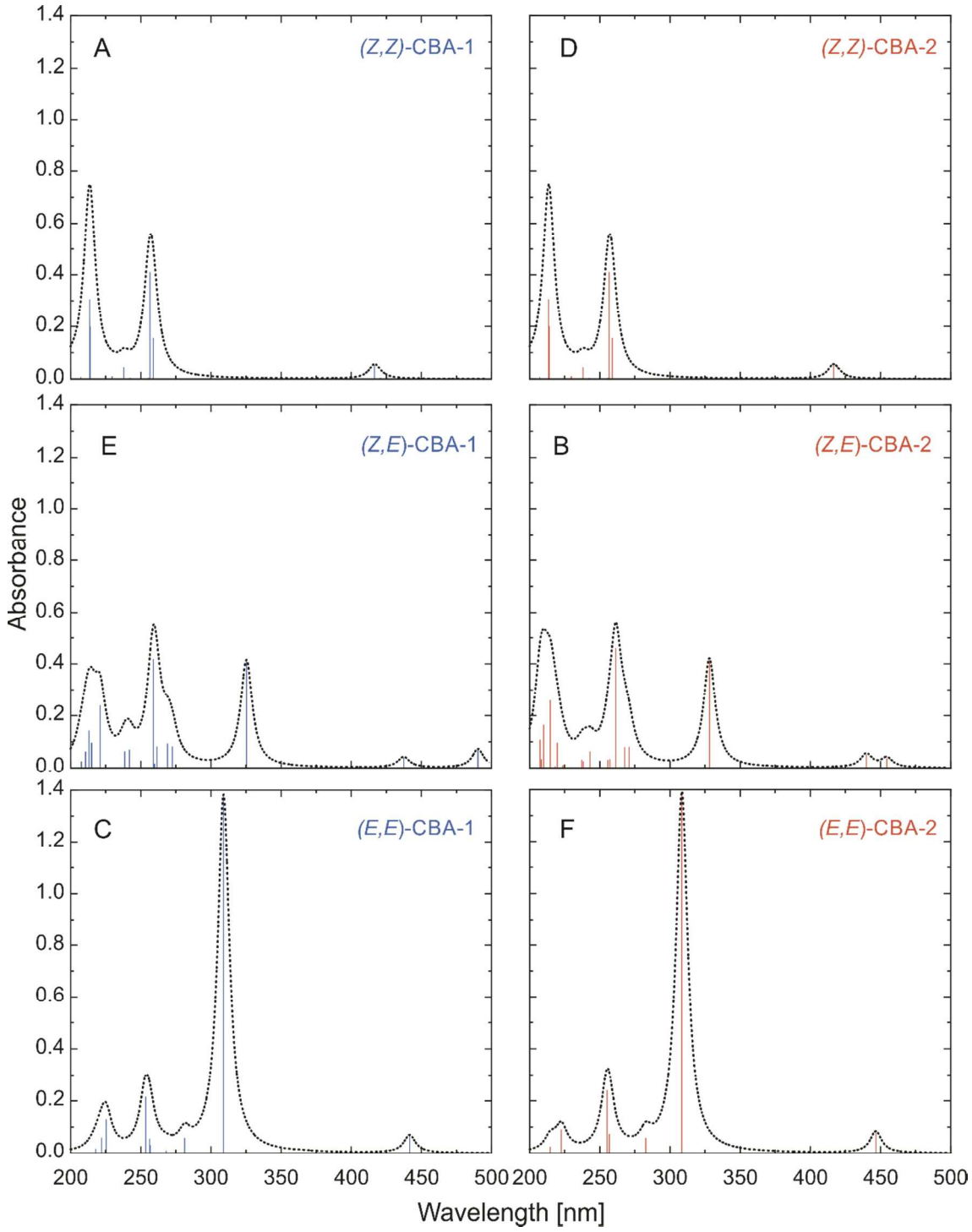

Figure S4. Calculated excitation energies for the different isomers of CBA and for the two stable ground state geometries – 1 and 2 (see Fig. S3).

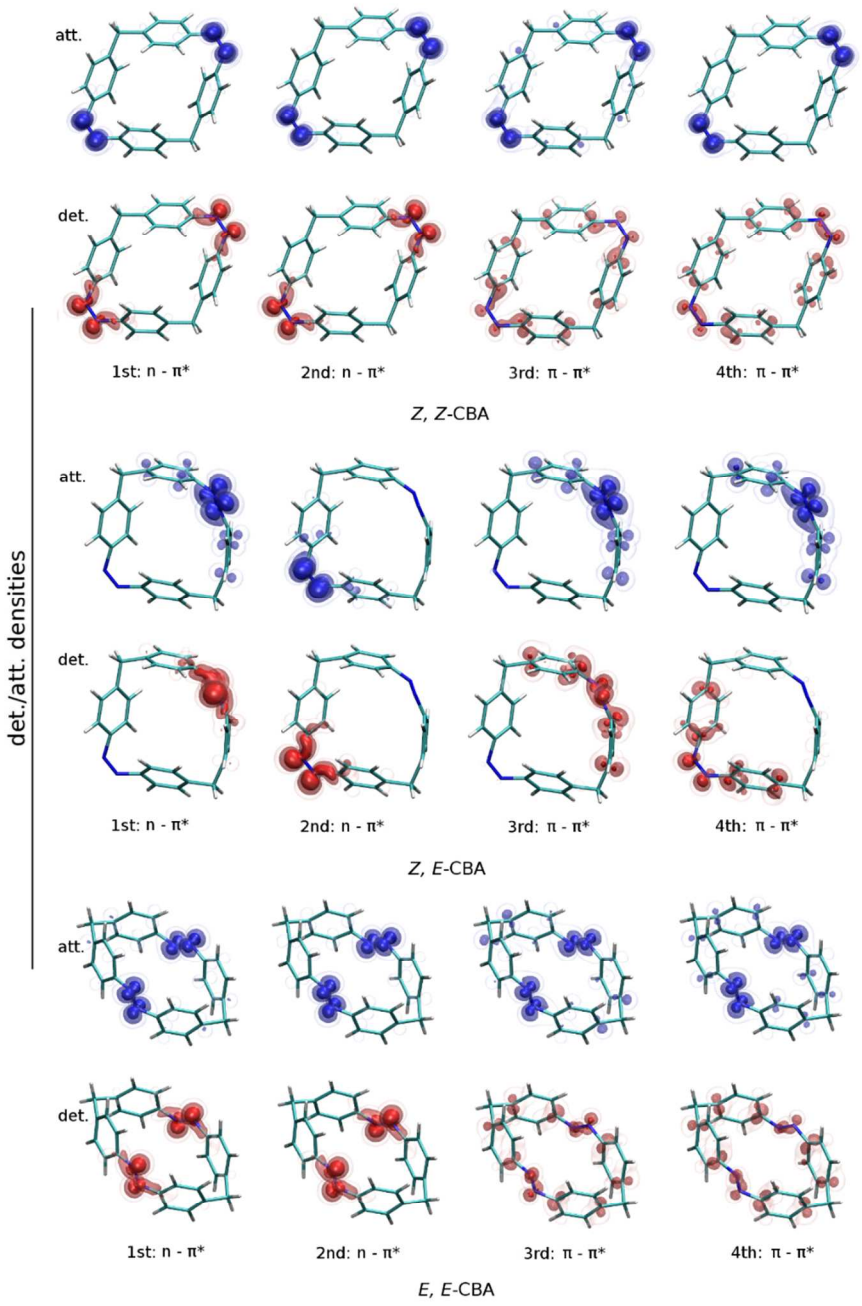

Figure S5. Detachment (red) and attachment (blue) densities for the lowest excited states at the TDDFT/BHLYP/6-31G* level of theory for the investigated CBA compound. The detachment density corresponds to that part of the density that is removed upon excitation, while the attachment density is the one that is added.

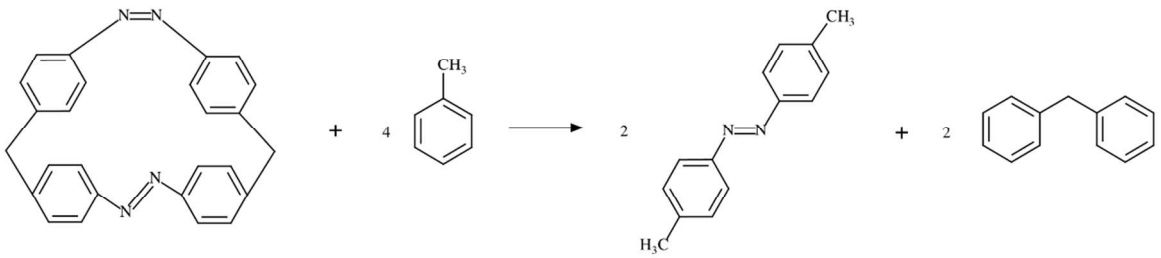

Figure S6. Isodesmic reaction used to calculate the strain energy in CBA, shown for the (*Z,E)*-isomer. Analogous reactions were considered for the *(Z,Z)*- and the *(E,E)*-isomers.

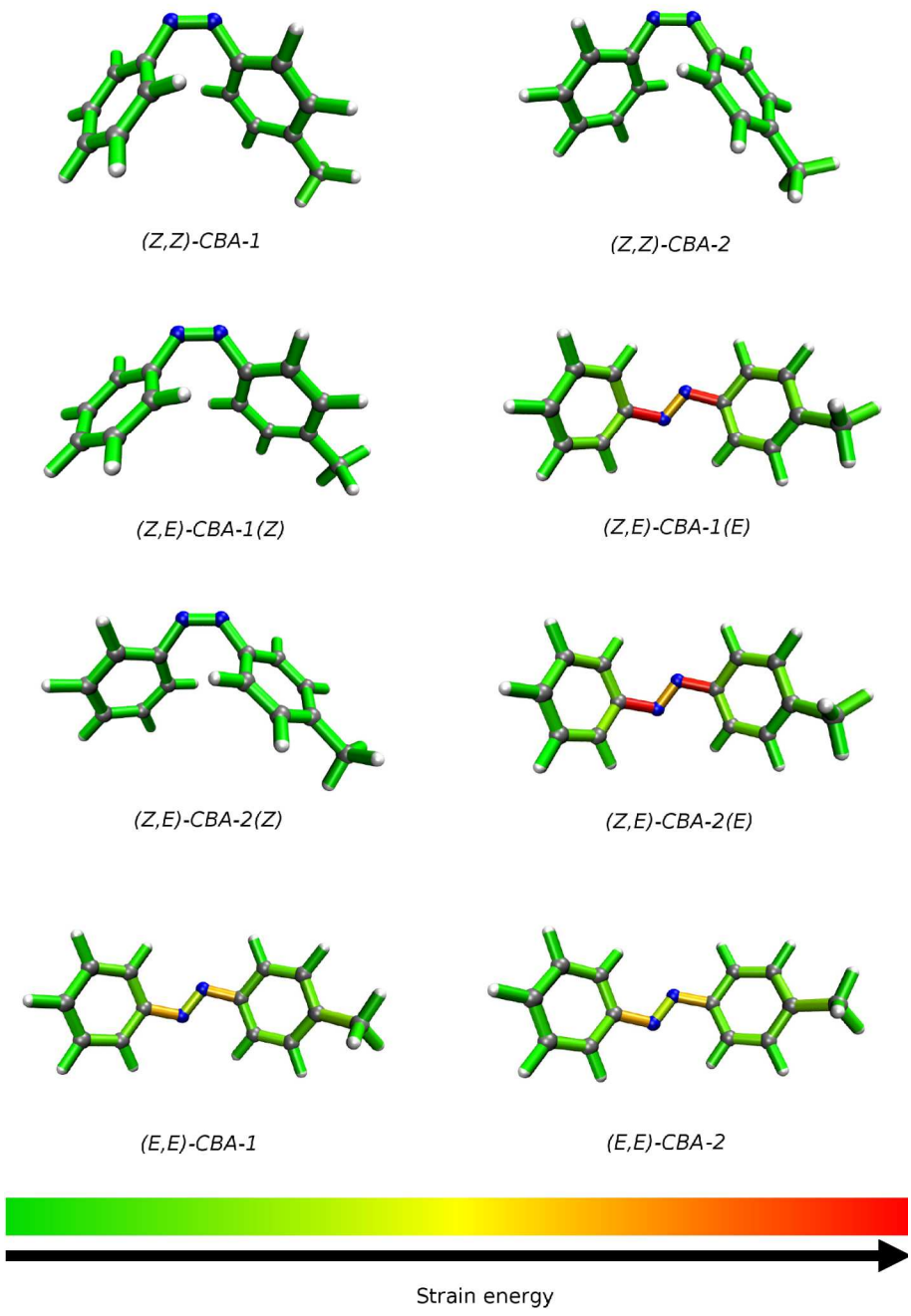

Figure S7. Color-coded representation of the total amount of strain energy in the different isomers of CBA. Only half of the molecules are shown (see text for explanation).

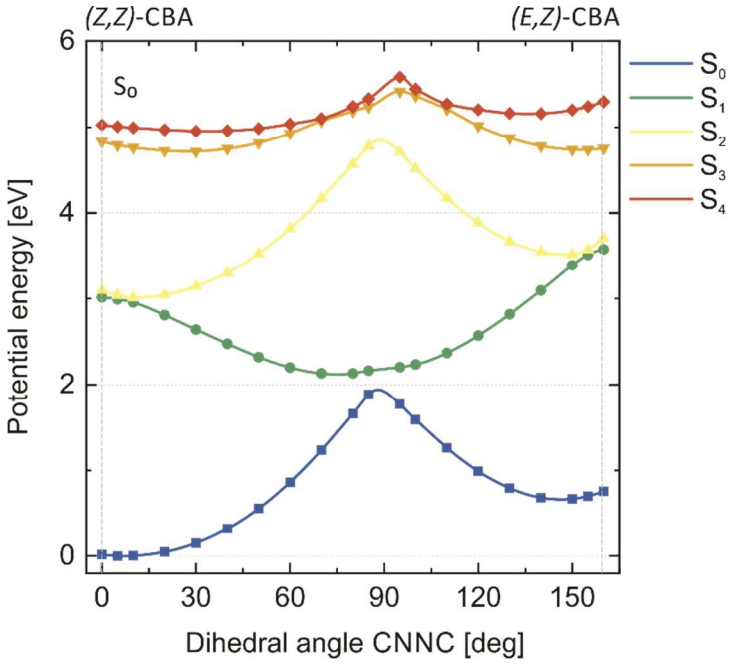

Figure S8. Potential energy curves for the torsion around one of the N═N double bonds in CBA-1 calculated for the S_0 optimized geometry at fixed values of the CNNC dihedral angle.

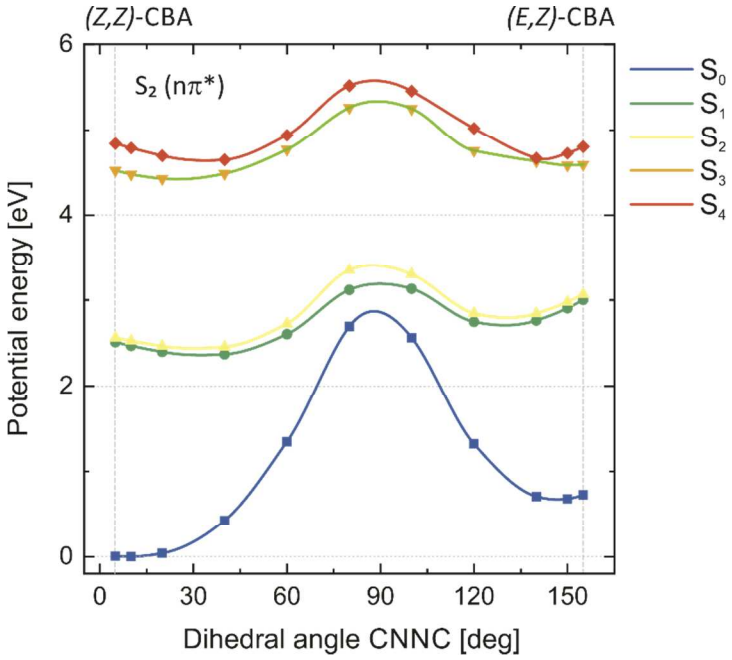

Figure S9. Potential energy curves for the torsion around one of the N═N double bonds in CBA-1 calculated for the S_2 optimized geometry at fixed values of the CNNC dihedral angle.

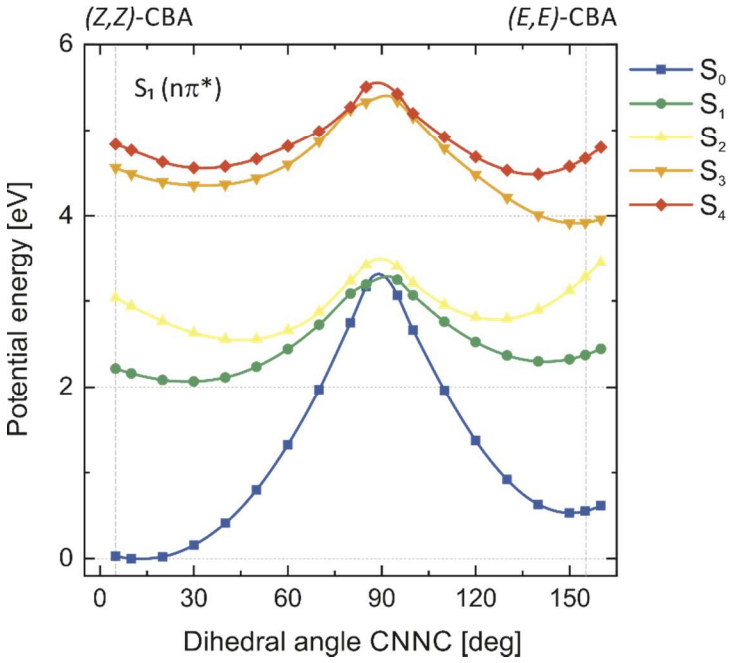

Figure S10. Potential energy curves for the concerted torsion around the two N═N double bonds in CBA-1 calculated for the S_1 optimized geometry at fixed values of the CNNC dihedral angle.